Ukrainian Journal of Ecology

Ukrainian Journal of Ecology, 2018, 8(3), 154-163

REVIEW ARTICLE

Reconstruction of compressive sensing-based SAR imaging using Nesterov's algorithm

A.E. Zadeh, B. Zanj, M. Nahvi

Department of Electrical Engineering, Faculty of Engineering, University of Guilan, 41635-3756, Rasht, Iran
E-mail: ahmadelect@gmail.com (or) zanj@guilan.ac.ir
Submitted: 01.05.2018. Accepted: 28.05.2018

Synthetic Aperture Radar (SAR) is a 2-D imaging technique. In this technique, to reconstruct high resolution images, wide bandwidth transmission signal and short length antenna are required and leading large data storage, high speed A/D converter (ADC) and short swath. To improve these drawbacks, using a recent developed theory known as compressive sensing (CS), it is possible to reconstruct high resolution image using undersampled data. This paper presents a new reconstruction algorithm based on Nesterov's algorithm. The simulation demonstrates promising results and indicates that the proposed algorithm has the advantage of high speed of convergence and accuracy.
Keywords: Synthetic aperture radar; compressive sensing; 1l minimization; Nesterov's algorithm

Introduction

SAR is an imaging technique that can produces 2D image. The main advantages of SAR are the capability of imaging during day and night and all weather conditions. Radar platform moves along scene and transmits pulses in a regular time interval (PRT) and record echoes, as shown in Figure 1.

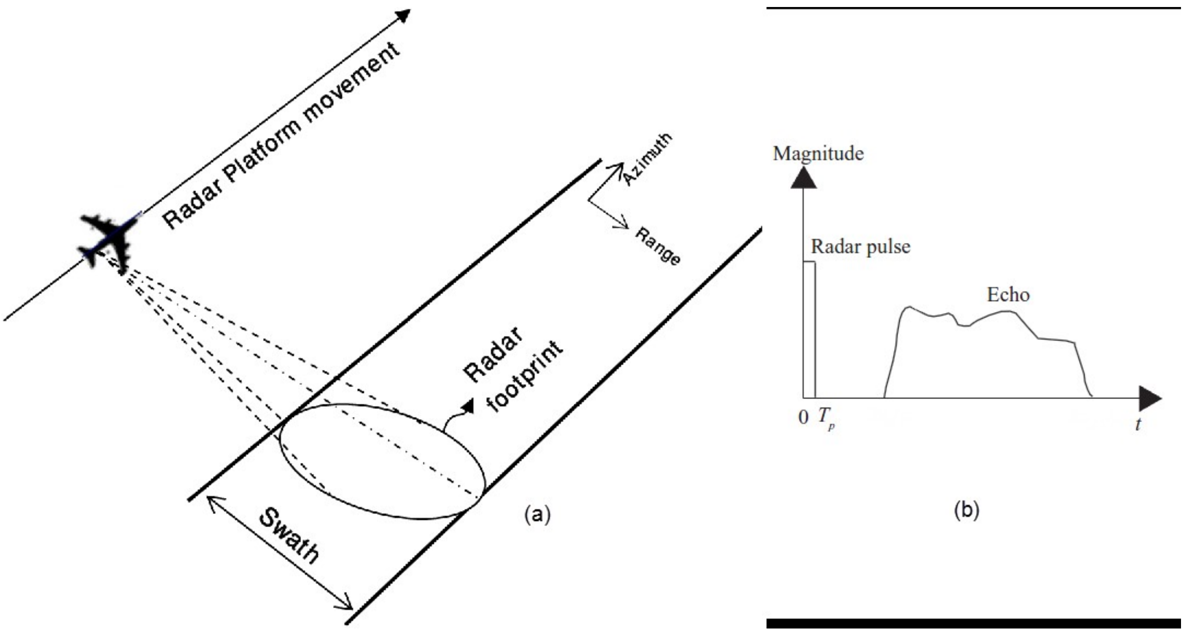

Figure 1. (a) SAR imaging geometry (b) Transmitted and received signal (Zyl, 2011).

Traditional radar imaging technique is Range Doppler Algorithm (RDA) based on match filtering (MF). In the RDA, wide bandwidth transmitted signal and short antenna length are necessary. The former gives high resolution image in the range direction and the latter improves Azimuth direction(Wang, 2008) and (Cumming & Wong, 2005). However, high resolution radar imaging needs large data storage, high speed ADC and resulting in shorter swath. Recently a new method known as Compressive Sensing (CS) has been introduced to reconstruct SAR image from few samples. In fact, these few measurements are linear projections of original signal. For accurate reconstruction, the signal must be sparse or compressible. Thus, CS can be considered as a solution to overcome the disadvantages of conventional RDA. R. Baraniuk et al. proposed CS-based SAR imaging(Baraniuk & Steeghs, 2007). In their system, transmitter is similar the conventional SAR imaging but MF and high-rate ADC in the receiver are replaced with law-rate ADC. The CS reconstruction algorithm has also been performed by greedy algorithms such as orthogonal matching pursuit (OMP) (Tropp & Gilbert, 2007), for example. In (Patel, Easley, Healy & Chellappa, 2010) has been shown that, unlike Baraniuk's approach, if radar transmits randomly generated pulses, there is no need to new hardware. In this method undersampling is however only performed in the azimuth direction. In (Xu, Pi & Cao, 2012), by transmitting random pulses and randomly sampled echoes, undersampling is performed in both dimensions. In (Wei, Zhang, Shi & Xiang, 2010), complete SAR raw data is reshaped into a vector and then randomly sampled. In (Jing, Shunsheng & Junfei, 2012), the CS technique is performed in 2-D image using only few samples. Since CS-based reconstruction take much more time and need large memory, instead of reconstruction whole scene in one process, in (JunGang, Thompson, Xiaotao, Tian & Zhimin, 2013) the whole scene is split into a set of small subscenes. The complete image can then be obtained by combining the reconstructed image of subscenes. To improve the reconstruction algorithm, this paper presents an efficient method based on Nestorv's algorithm (Nesterov, 2005). The implementation of this algorithm indicates its promising performance on noisy measurments. The results demonstrate speed and good accuracy of the new method comparing to those of conventional reconstructions such as fast iterative shrinkage thresholding algorithm(FISTA) for linear inverse problem (Beck & Teboulle, 2009), spectral projected gradient(SPGL1) (van den Berg & Friedlander, 2008) and gradient projection for sparse reconstruction (GPSR) (Figueiredo, Nowak & Wright, 2007). To reduce the length of the paper, there are no details of these algorithm in this paper.

In what follows CS theory is reviewed in the next section. In section 3, Nesterov's algorithm, its acceleration method and proposed CS reconstruction based on Nesterov's algorithm are presented. SAR imaging and CS-based SAR imaging is introduced in section 4. In section 5 and 6, simulation results and conclusion remarks are given, respectively.

Basic theory of CS

Shanon-Nyquist theory states that to reconstruct original signal by discrete samples, sampling frequency must be more than twice the maximum frequency of the signal. But based on the CS theory, if signal is sparse or has a spars representation on some basis, it is possible to reconstruct signal with few linear measurements. Suppose that x (n × 1 vector) has spars representation on $\{\Psi_{1,}......,\Psi_N\}$ basis. i.e., it can be expressed as:

$$X=\Psi_{\alpha}, \qquad (1)$$

where Ψ is a matrix where it's columns are $\{\Psi_{1,}......,\Psi_N\}$ and α is an N × 1 vector with up to k nonzero elements. Using equation (1), measurement vector y is expressed by:

$$y= \phi x= \phi\Psi\alpha= \Theta\alpha\ , \qquad (2)$$

where ϕ is an M × N measurement matrix, and usually M × N, and Θ × ϕΨ . Since l_0-norm counts the number of non-zero entries, the reconstruction of the original signal can be obtained by solving the following problem:

$$\hat{\alpha} = \arg\min \|\alpha\|_{l_0}\ , \text{ Subject to } y=\Theta\alpha, \qquad (3)$$

problem (3) is an NP- hard problem. In (Candes & Tao, 2005) showed it has been shown that if Θ has restricted isometry property(RIP), then (3) can be replaced by the following convex problem:

$$\hat{\alpha} = \arg\min \|\alpha\|_{l_1}\ , \text{ Subject to } y=\Theta\alpha, \qquad (4)$$

which can be solved. RIP has been defined as:

$$1-\varepsilon \le \frac{\|\Theta\alpha\|_{l_2}}{\|\alpha\|_{l_2}} \le 1+\varepsilon,\ \varepsilon \in (0,1) \qquad (5)$$

And conceptually states that Θ preserve the distance between any pair of spars vectors.

But RIP check of a matrix is a combinatorial search. Fortunately if the entries of ϕ are selected independent and identically distributed sub-gaussian random, it has RIP with high probability with M ≥ c (k log (N/K)) measurements.

For noisy measurement, it is proven (Eldar & Kutyniok, 2012) that if measurement matrix satisfies RIP, the uniqueness for solution has been guaranteed and reconstruction formula is:

$$\hat{\alpha} = \arg\min \|\alpha\|_{l1},\ \textit{Subject to}\ ,\|y=\Theta\alpha\|_{l_2} \le \varepsilon \qquad (6)$$

where ε is the amount of noise in measured data.

Generally, there are three class of CS reconstruction, which has been described in the following (Eldar & Kutyniok, 2012):

l1 minimization based algorithms: These algorithms solve a convex optimization problem and provide an accurate reconstruction. Another advantage is using few measurements, but the reconstruction is computationally complex. The Nestrov's algorithm and other algorithm which are used in this paper are in this category.

Greedy based algorithms: These algorithms solve the problem by searching the answer iteratively. They are fast and have low computational complex. MP and OMP are some example of greedy algorithm.

Approximate message passing algorithms: This approach uses an iterative method and it is useful to solve large-scale regularized regression problems. Specially LASSO and BPDN in CS reconstruction problems. In addition to equivalent sparsity-undersampling tradeoff, it is fast in compared with l1-minimization based algorithms.

Nesterov's algorithm

Nesterov (Nesterov, 2005) uses smoothing and gradient methods to implement 1st-order techniques to solve optimization problems. Nesterov's algorithm has been used to minimize non-smooth functions. An advantage of Nesterov's algorithm is exploiting smoothing techniques which makes it applicable on many types of minimization problems. Two further benefits of this algorithm are controllable convergence using a smoothing parameter , and also acceptable accuracy. This means that by increasing speed, the accuracy is not deducted. Nesterov (Nesterov, 1983) presented a method for convex minimization and smooth function f over the convex set Q_p, that is:

$$\min_{x\in Q_p} f(x) \qquad (7)$$

where Q_p is primal feasible set, and f is differentiable and Lipschitz; that is for any x,y ϵ Q_p:

$$\left\|\nabla f(x)-\nabla f(y)\right\|_{l_2} \le L\left\|x-y\right\|_{l_2}, \qquad (8)$$

where L is Lipschitz constant.
To minimize non-smooth function f, Nesterov demonstrated that the following optimization problem can be solved (Nesterov, 2005):

$$f(x)=\max_{u\in Q_d}\langle u, Ax\rangle, \qquad (9)$$

where, Q_d is dual feasible set and A is a transform from Qp to Qd. Suppose d(u) is a prox-function on Q_d, therefore d(u) is strongly convex and continuous, and prox-center is defined as:

$$u_0=\min_u\left\{d(u), u\in Q_d\right\} \qquad (10)$$

hence d(u) is equal to:

$$d(u)\ge\frac{1}{2}\sigma\left\|u-u_0\right\|_{l_2}, \qquad (11)$$

,

where σ is convexity parameter. Thus smooth function for f will be defined as:

$$f_\mu(x)=\max_u\left\{\langle Ax,u\rangle-\mu d(u)\right\} \qquad (12)$$

In (12) μ is positive and smoothing parameter. And the gradient of smooth function is equal to:

$$\nabla f_\mu(x)=A^*u_\mu(x), \qquad (13)$$

where is an optimal solution of (12) and is Hermitian Conjugate of A. Nesterov also proved that Lipschitz constant for f_μ is equal to:

$$L_\mu=\frac{1}{\mu\sigma}\left\|A\right\|^2 \qquad (14)$$

The stages of Nesterov's algorithm for minimization of non-smooth function are given as below:

1. Initialize x_0; for k ≥ 0 do,
2. Compute $f(x_k)$ and $\nabla f(x_k)$.
3. Find $y_k=\arg\min_{y\in Q_p}\left\{\langle\nabla f(x), y-x\rangle+\frac{1}{2}L\left\|y-x\right\|^2\right\}$.
4. Find $Z_k=\arg\min_{x\in Q_p}\left\{\frac{L}{\sigma}d(x)+\sum_{i=0}^{k}\frac{i+1}{2}\left[f(x_i)+\langle\nabla f(x_i), x-x_i\rangle\right]\right\}$.
5. Set $x_{k+1}=\frac{2}{k+3}z_k+\frac{k+1}{k+3}y_k$.
6. If given criterion is satishfied, then stop.

Nestrov proved that converges with rate of:

$$f(y_k)-f(x^*)\le\frac{4Ld(\mathrm{x}^*)}{\sigma(k+1)(k+2)}, \qquad (15)$$

Where is an optimum value of x. Using equations (12), (14) and (15) it can be understood that to improve the accuracy in smoothing (12), smaller μ is needed while in (14) and (15) larger μ increases the convergence rate. In fact, μ is a trade-off between accuracy and speed of algorithm.

Accelerating Nesterov's algorithm using continuation

In (Becker, Bobin & Candès, 2011), by continuation and trade-off between accuracy and speed by selection of μ, a continuation algorithm for Nesterov 's method is presented which increases the rate of convergence. The basic idea of this algorithm is initializing μ with large value that is leading to increase in speed of algorithm and then reducing the value of μ as algorithm advances. This is proceeding by Nestrov's algorithm, to increase the accuracy. Accelerating algorithm is as below (Becker et al., 2011);

1. Initialize μ0, x0 and number of continuation step T. for t=1,2,. . .,T.
2. Apply Nestrov's algorithm with μ=μt and $x_0 = x_{\mu^{(t-1)}}$.
3. Decrease the value of μ; $\mu^{(t+1)} = \gamma\mu^{(t)}$ with γ <1.
4. Stop when desired value of μ is reached.

CS reconstruction using Nesterov's algorithm

The reconstruction problem in CS is:

$$\arg\min \|x\|_{l_1} \text{ ,Subject to } \|y - \Phi X\| \le \varepsilon \text{ (16)}$$

But $f(\mathrm{x}) = \|x\|_{l_1}$ is non-smooth function, therefore Nesterov's algorithm can be adapted to solve (16) (Becker et al., 2011):

$$f(\mathrm{x}) = \|x\|_{l_1} = \max_{u \in Q_d} \langle u, x \rangle, \text{ where, } \mathrm{Q}_d = \{u : \|u\|_\infty \le 1\} \qquad (17)$$

Thus smooth approximation of f(x) is:

$$f_\mu(x) = \max_{u \in Q_d} \langle u, x \rangle - \mu d(u) \qquad (18)$$

Assume the value of prox-center is equal to zero and σ =1, then:

$$f_\mu(x) = \max_{u \in Q_d} \langle u, x \rangle - \frac{\mu}{2}\|u\|_{l_2}^2 \qquad (19)$$

Since (19) is a smooth function, Nesterov's algorithm can be used to find its solution.

For noisy measurements y=ϕX+n, which is measurement matrix and n is additive noise, there are two approaches to reconstruct signal:

1) Synthesis approach: $$\arg\min \|\alpha\|_{l_1}, \ \|y - \Phi\Psi\alpha\| \qquad (20)$$

2) Analysis approach: $$\arg\min \|X\|_{l_1}, \ \|y - \Phi X\| \qquad (21)$$

The proposed algorithm in this paper can solve both of above problems, and it is one of few algorithms which can solve Analysis (Becker et al., 2011). By using Analysis problem, in (Becker et al., 2011) they used a novelty to decrease cost of algorithm. In many CS problems, the measurement matrix ϕ is a submatrix of unitary transformation U that can be written as:

Φ =RU, UU*=U*U=I (22)

Where R is an m × n subsampling operator. To apply novelty, the following change of variable has been done:

$$\tilde{x} = Ux, \tilde{f}(\tilde{\mathrm{x}}) = \mathrm{f}(\mathrm{U}^* \tilde{\mathrm{x}}) = f(\mathrm{x}) \qquad (23)$$

Therefore, the analysis problem will be:

$$\arg\min \tilde{\mathrm{f}}(\tilde{x})_{\text{Subject to}} \|\mathrm{y} - \mathrm{R}\tilde{x}\| \le \varepsilon \quad (24)$$

The advantage of this change of variable is applying of U and U* once per iteration, while U and U* is the dominant cost of algorithm. For example, suppose U is an FFT, then the cost per iteration will be two FFTs.

CS-based SAR imaging

Transmitted signal by radar is a Linear Frequency Modulation (LFM) pulse(Wang, 2008):

$$S_T(\mathrm{t}) = \mathrm{rect}\left(\frac{t}{T_p}\right) e^{(\mathrm{j}2\pi \mathrm{f_c t} + \mathrm{j}\pi\alpha \mathrm{t}^2)} \qquad (25)$$

(25)

where rect(t) is rectangular function, fc is carrier frequency, Tp is pulse width and α is LFM chirp rate. As radar platform moves along flight (Azimuth) direction transmits pulses in equal time interval (PRT) and records echoes, so the received signals is equal to sum of echoes:

$$\mathrm{S_R}(\eta, t) = \iint_D \sigma(x,y)\, rect\left(t - \frac{2R(\eta,x,y)}{c}\right) e\left[j2\pi f_c\left(t - \frac{2R(\eta,x,y)}{c}\right) + j\pi\alpha\left(t - \frac{2R(\eta,x,y)}{c}\right)\right] dxdy \qquad (26)$$

(26)

where R(η,x,y) is the slant range from target located at (x,y) to radar at slow time *η*, t is fast-time, D is imaging area and *σ* (x,y) is reflectivity coefficient, x is range and y azimuth directions. To illustrate radar data in discrete domain, imaging area is considered discrete, as shown in Figure 2.

Figure 2. SAR Geometry in Discrete Spatial Domain.

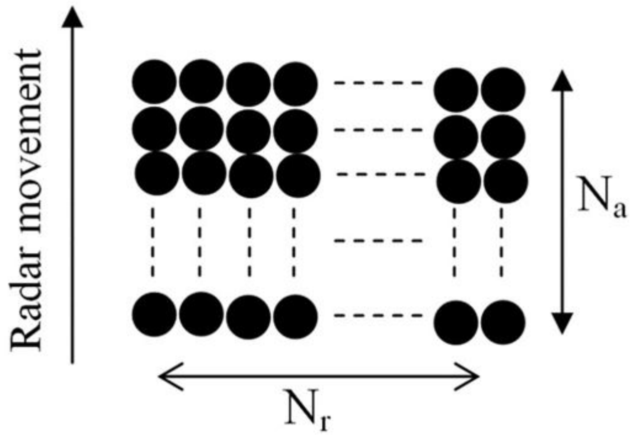

This can be expressed as:

$$\Sigma=\begin{bmatrix}\sigma(1,1) & \sigma(1,2) & \cdots & \sigma(1,N_r)\\ \sigma(2,1) & \sigma(2,2) & \cdots & \sigma(2,N_r)\\ \vdots & \vdots & \cdots & \vdots\\ \sigma(N_a,1) & \sigma(N_a,2) & \cdots & \sigma(N_a,N_r)\end{bmatrix} \qquad (27)$$

where Σ is reflectivity coefficient of all targets, Na is the number of targets in azimuth direction, Nr is the number of targets in range direction and σ (i,j) is reflectivity coefficient for $(i,j)^{th}$ entry of the Σ. To implement CS scheme, the reflectivity coefficients of targets can be reshaped in a vector as:

$$\boldsymbol{\sigma}=\left[\sigma(1,1) \;\; \cdots \;\; \sigma(N_a,1) \;\; \cdots \;\; \sigma(1,N_r) \;\; \cdots \;\; \sigma(N_a,N_r)\right]^T \qquad (28)$$

where **σ** is an N × 1 vector and N=Na × Nr. Then, discrete form of equation (26) is expressed as:

$$S_R(\eta,t)=\sum_{k=0}^{N}\sigma_k e^{\left[j2\pi f_c\left(t-\frac{2R_{\eta,k}}{c}\right)+j\pi\alpha\left(t-\frac{2R_{\eta,k}}{c}\right)^2\right]} \qquad (29)$$

In (24) Rη, k is slant range of kth target to the radar platform at slow time η, which is equal to:

$$R_{\eta,k}=\sqrt{R_0^2+(v\eta-y_k)^2} \qquad (30)$$

where $R_0=\sqrt{x^2+H^2}$, v and H are the velocity and height of the radar platform, respectively.

By using $R_{\eta,k}=\sqrt{R_0^2+(v\eta-y_k)^2}\approx R_0+\frac{(v\eta-y_k)^2}{2R_0}$, and its substituting in the equation (29), $S_R(\eta,t)$ is expressed by:

$$S_R(\eta,t)=\sum_{k=0}^{N}\sigma_k e^{\left[j\pi\alpha\left(t-2\frac{R_0+\left(\frac{v\eta-y_k}{2R_0}\right)^2}{c}\right)^2-j\pi f_c\frac{R_0+\left(\frac{v\eta-y_k}{2R_0}\right)^2}{c}\right]}=\sum_{k=0}^{N}\sigma_k e^{-j\varphi_k(\eta,t)} \qquad (31)$$

The linear model of SAR raw data is given by:

$S_R=A\sigma+n$ (32)

where n is additive noise, A is an N × N SAR echo signals measurement matrix:

$A=[a_1(\eta,t), a_2(\eta,t),\ldots, a_k(\eta,t),\ldots,a_N(\eta,t)]$, (33)

$$a_k(\eta,t)=\left[e^{-j\varphi_k(1,1)},e^{-j\varphi_k(1,2)},\cdots,e^{-j\varphi_k(1,N_r)},e^{-j\varphi_k(2,1)},\cdots,e^{-j\varphi_k(N_a,N_r)}\right]^T \qquad (34)$$

As mentioned earlier in this paper, sparsity is a pre-requirement to use CS scheme. So if reflectivity coefficients are not sparse, it is possible to get a sparse approximation as:

$\sigma=\Psi\alpha$ (35)

Therefore (32) can be expressed as:

$$S_R=A\psi\alpha+n \quad (36)$$

To perform CS technique it is required to randomly choose few samples of S_R and the rows of A must be chosen corresponding to the selected samples of S_R . Thus, if S'_R is undersampled S_R and A' is undersampled A, then the measurements in CS will acquire by:

$$S'_R=A'\alpha+n=\phi A\alpha+n=\phi A\Psi\alpha+n=\Theta\alpha+n \quad (37)$$

An approach for determination of measurement matrix is randomly choosing of M rows of an N×N Identity matrix. The targets will then be reconstructed by:

$$\arg\min\|\boldsymbol{\alpha}\|_{l_1} \text{ Subjected to } \|S'_R-\Theta\alpha\|_{l_2}<\varepsilon \quad (38)$$

Simulation trials

In this paper the SAR signal was synthetically simulated and its parameters were f_c=1 GHz, BW= 30 MHz, H=5000 m, v=100 m/s, T_p=10 µs, PRF=58 Hz, and L=4 m. The imaging area contained 5 point targets. The area was constructed by Nr samples in the range direction and Na samples in the azimuth, consequently the whole samples were equal to N= $N_r \times N_a$. To perform CS scheme, SAR raw data was multiplied by the orthogonal Hadamard matrix and then the column of resulting matrix randomly permuted. To acquire measurements y, M rows are selected from N rows (M<N) and therefore the undersampled measurements y and measurement matrix Φ are known. The simulation trials have been performed in "Intel corei7 Processor" with 8 GB RAM.

Simulations results on the synthetic data were then compared with those of conventional methods. Figure 3 indicates that the area is partitioned in and thus N= 524288 total number of samples with 5 points targets. Reconstruction of noisy raw data was performed by several state-of-the-art approaches consist of FISTA, SPGL1, GPSR and Nesterov's algorithm. To verify the performance of the new algorithm, SNR for CS measurement were varied, and then Mean Square Error (MSE) and elapsed time for all methods were determined and compared, as shown in Table 1 and 2. As inferred, Nestrov's algorithm has great performance in elapsed time and MSE, especially in comparison with GPSR. In (Figueiredo et al., 2007), it is shown GPSR is faster than OMP and has smaller MSE. Using the results of Table 1 and 2 it can thus be concluded that Nestrov's algorithm is superior to OMP.

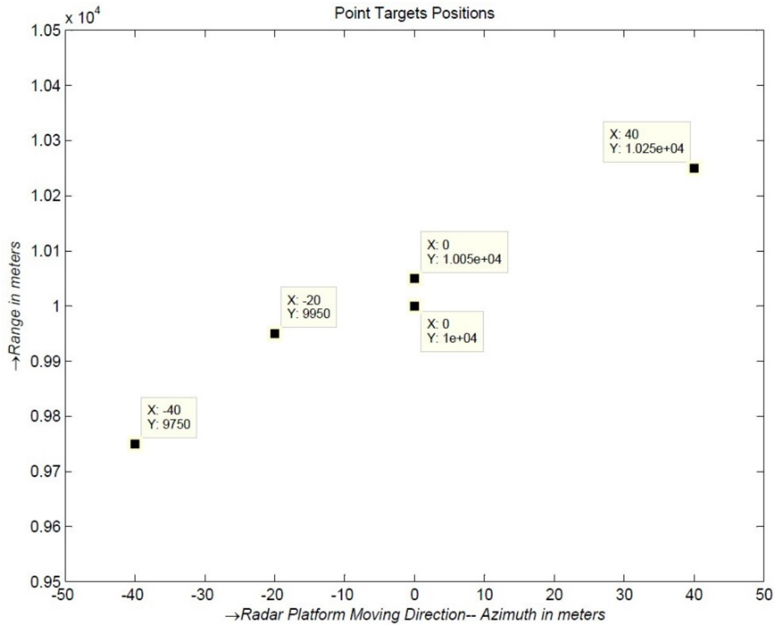

Figure 3. Simulated scene with 5 point targets.

Moreover, in the results of the Nestrov's algorithm there are no significant changes when the SNR is increased. The reason for this can be explained by the value of ε in (34), $\varepsilon \approx \sqrt{m}\,\sigma$ (Elad, 2010), where σ^2 is noise variance and m is number of measurements. Therefore by increasing SNR, and will be decreased. In other word, more appropriate fitting is expected; hence the convergence of the algorithm takes more time.

Table 1. Elapsed time in solving l1 optimization problem using four distinct Optimization methods for different Signal to Noise ratio.

SNR(dB)	10(dB)	20(dB)	30(dB)	40(dB)	50(dB)	60(dB)	70(dB)	80(dB)	90(dB)	100(dB)
	Time(s)									

Nesterov's algorithm	190.69(s)	129.22(s)	102.81(s)	118.72(s)	145.95(s)	176.34(s)	238.45(s)	205.51(s)	253.98(s)	177.53(s)
FISTA	152.92(s)	145.44(s)	309.73(s)	319.36(s)	421.26(s)	472.26(s)	685.33(s)	2235.62 (s)	2256.69 (s)	3259.42 (s)
SPGL1	138.11(s)	168.67(s)	405.58(s)	533.06(s)	999.33(s)	1136.76 (s)	1388.81 (s)	1481.87 (s)	1605.31 (s)	2908.05 (s)
GPSR	4940.08 (s)	6401.5(s)	5864.03 (s)	5941.27 (s)	5528.7(s)	6041.53 (s)	5700.76 (s)	5205.67 (s)	5156.72 (s)	5391.72 (s)

Table 2. MSE in solving l1 optimization problem using four distinct Optimization methods for different Signal to Noise ratio.

SNR(dB)	**10(dB)**	**20(dB)**	**30(dB)**	**40(dB)**	**50(dB)**	**60(dB)**	**70(dB)**	**80(dB)**	**90(dB)**	**100(dB)**
	MSE									
Nesterov's algorithm	0.15044	0.031751	0.00788	0.00328	0.002502	0.002431	0.002443	0.002517	0.002574	0.00276
FISTA	0.18492	0.026021	0.00757	0.02472	0.004163	0.003783	0.003336	0.003412	0.003418	0.00342
SPGL	0.06235	0.02082	0.0074	0.00399	0.003465	0.003435	0.003446	0.003432	0.003442	0.00346
GPSR	0.18869	0.026747	0.00781	0.0257	0.00472	0.004235	0.003559	0.003513	0.003409	0.00334

To observe the impact of number of sample on the performance of these algorithms, number of measured samples has been changed and the reconstruction results were compared. Table 3 and 4 indicate the elapsed time and MSE of various methods, respectively. By comparison of the results in the tables it can clearly be deduced that Nestrov's algorithm gives better performance.

Table 3. Elapsed time in solving l1 optimization problem using four distinct Optimization methods for different percentage of full Sample.

Percentage Of Full Sample	**0.3**	**0.4**	**0.5**	**0.6**	**0.7**
	Time(s)				
Nesterov's algorithm	103.7(s)	97.37(s)	92.94(s)	88.83(s)	88.72(s)
FISTA	309.83(s)	131.36(s)	236.26(s)	121.72(s)	206.37(s)
SPGL	405.33(s)	335.28(s)	318.83(s)	353.69(s)	379.2(s)
GPSR	5855.45(s)	6740.52(s)	7705.81(s)	7256.33(s)	7562.68(s)

Table 4. MSE in solving l1 optimization problem using four distinct Optimization methods for different Percentage Of full sample.

Percentage Of Full Sample	**0.3**	**0.4**	**0.5**	**0.6**	**0.7**
	MSE				
Nesterov's algorithm	0.00788	0.0053	0.00392	0.03004	0.002365
FISTA	0.00757	0.04414	0.005969	0.017677	0.011315
SPGL	0.0074	0.00493	0.00362	0.002694	0.002124
GPSR	0.00781	0.04542	0.006253	0.018284	0.011754

The simulation of point targets imaging was also performed by RDA and CS-based technique. It should be noted that the CS-based reconstruction was carried out by Nesterov's Algorithm. The imaging area was partitioned in 64 × 64 and N=4096. Figure 4 shows simulated targets. In our simulations the number of undersampled measurements was M=0.3 N ≈ 1229 samples.

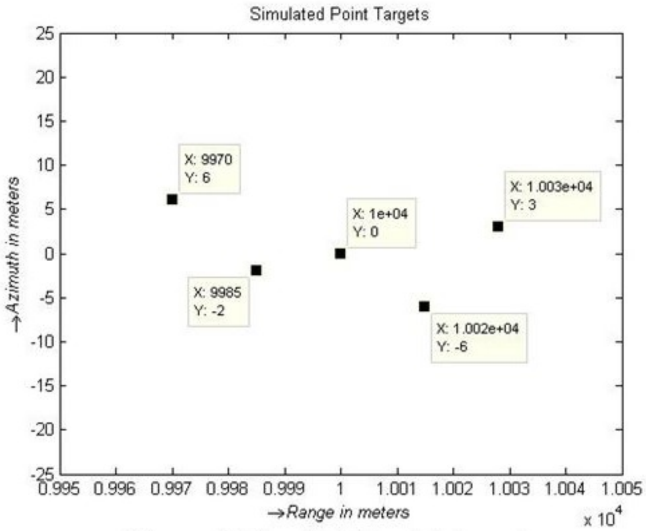

Figure 4. Simulated point targets.

The reconstructed point targets using RDA with complete set of samples, N=4096, is shown in Figure 5. In this figure, darker points are locations of point targets and brighter ones are side-lobes.

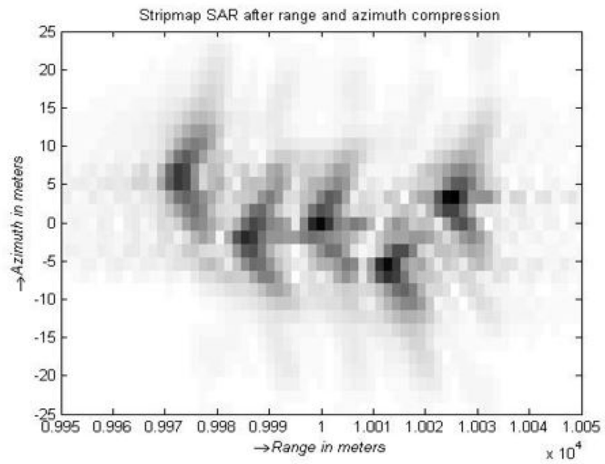

Figure 5. Stripmap SAR imaging by RDA and complete set of samples, N=4096.

Figure 6 also shows 3dB contour of reconstructed targets shown in Figure 5. Finally Figure 7 illustrates the reconstructed point targets by CS reconstruction using Nesterov's algorithm. In this reconstruction only M=1229 samples were used. Comparison of Figure 5 and Figure 7 indicates that the targets can precisely be recognized from each other in Figure 7.

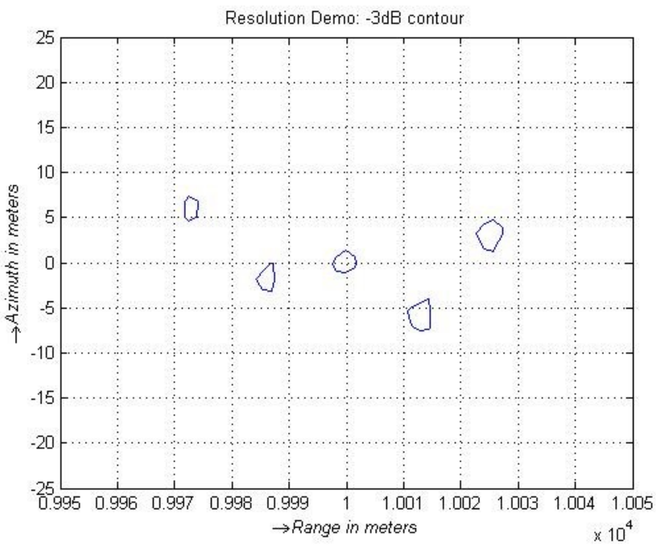

Figure 6. 3dB contour for reconstructed point targets using Range Doppler Algorithm.

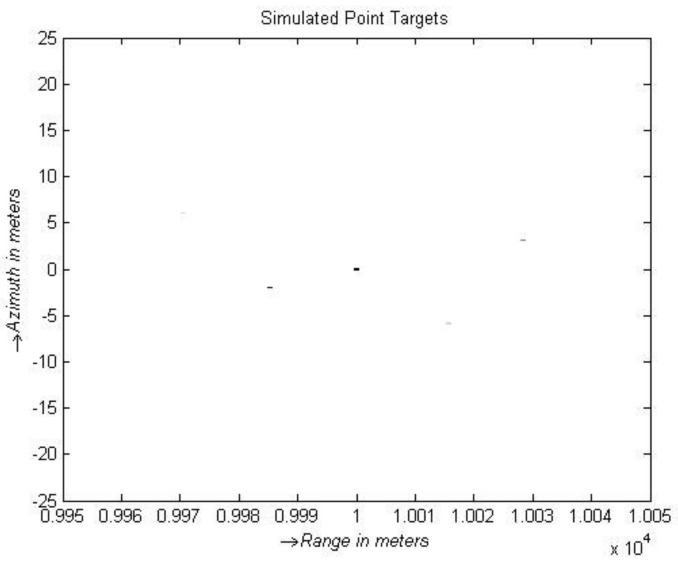

Figure 7. Stripmap SAR Imaging using Nesterov's Algorithm with only M=1229 samples.

Conclusion

The paper presented a new CS-based SAR image reconstruction using Nesterov's optimization algorithm. In conventional MF-based SAR, to obtain high resolution images, large data storage, high speed ADC converter and short swath are needed. In the new reconstruction algorithm, the performance of existing CS-based algorithm improved using Nesterov's algorithm. The main advantage of the presented method is reconstruction of high resolution image with significant reduction in the number of required data. The simulation of the new algorithm demonstrated promising results. It resulted in high resolution image with less side lobes, while it improves the speed and accuracy of reconstruction process. The simulation results demonstrated that, in comparison to three state-of-the-art methods, the proposed method has fast convergence and accuracy.

References

Baraniuk, R., & Steeghs, P. (2007). Compressive Radar Imaging. Paper presented at the Radar Conference, 2007 IEEE.

Beck, A., & Teboulle, M. (2009). A Fast Iterative Shrinkage-Thresholding Algorithm for Linear Inverse Problems. SIAM Journal on Imaging Sciences, 2(1), 183-202. doi:doi:10.1137/080716542

Becker, S., Bobin, J., & Candès, E. (2011). NESTA: A Fast and Accurate First-Order Method for Sparse Recovery. SIAM Journal on Imaging Sciences, 4(1), 1-39. doi: 10.1137/090756855

Candes, E. J., & Tao, T. (2005). Decoding by linear programming. IEEE Transactions on Information Theory, 51(12), 4203-4215. doi:10.1109/TIT.2005.858979

Cumming, I. G., & Wong, F. H. (2005). Digital Processing of Synthetic Aperture Radar Data: Algorithms and Implementation: Norwood, MA: Artech House.

Elad, M. (2010). Sparse and Redundant Representations: From Theory to Applications in Signal and Image Processing: Springer Publishing Company, Incorporated.

Eldar, Y. C., & Kutyniok, G. (2012). Compressed Sensing: Theory and Applications: Cambridge University Press.

Figueiredo, M. A. T., Nowak, R. D., & Wright, S. J. (2007). Gradient Projection for Sparse Reconstruction: Application to Compressed Sensing and Other Inverse Problems. IEEE Journal of Selected Topics in Signal Processing, 1(4), 586-597. doi:10.1109/jstsp.2007.910281

Jing, L., Shunsheng, Z., & Junfei, C. (2012). Two-dimensional random sparse sampling for high resolution SAR imaging based on compressed sensing. Paper presented at the Radar Conference (RADAR), 2012 IEEE.

JunGang, Y., Thompson, J., Xiaotao, H., Tian, J., & Zhimin, Z. (2013). Segmented Reconstruction for Compressed Sensing SAR Imaging. Geoscience and Remote Sensing, IEEE Transactions on, 51(7), 4214-4225. doi:10.1109/tgrs.2012.2227060

Nesterov, Y. (1983). A method of solving a convex programming problem with convergence rate O ($1/k^2$). Soviet Mathematics Doklady, 27(2), 372-376.

Nesterov, Y. (2005). Smooth minimization of non-smooth functions. Mathematical Programming, 103(1), 127-152. doi:10.1007/s10107-004-0552-5

Patel, V. M., Easley, G. R., Healy, D. M., Jr., & Chellappa, R. (2010). Compressed Synthetic Aperture Radar. Selected Topics in Signal Processing, IEEE Journal, 4(2), 244-254. doi:10.1109/jstsp.2009.2039181

Tropp, J. A., & Gilbert, A. C. (2007). Signal Recovery From Random Measurements Via Orthogonal Matching Pursuit. Information Theory, IEEE Transactions on, 53(12), 4655-4666. doi:10.1109/tit.2007.909108

van den Berg, E., & Friedlander, M. (2008). Probing the Pareto frontier for basis pursuit solutions. SIAM Journal on Scientific Computing, 31, 890-912. doi: 10.1137/080714488

Wang, B. C. (2008). Digital signal processing techniques and applications in radar image processing: John Wiley.

Wei, S. J., Zhang, X. L., Shi, J., & Xiang, G. (2010). Sparse reconstruction for SAR imaging based on compressed sensing. Progress In Electromagnetics Research, 109, 63-81.
Xu, J., Pi, Y., & Cao, Z. (2012). Bayesian compressive sensing in synthetic aperture radar imaging. Radar, Sonar & Navigation, IET, 6(1), 2-8. doi:10.1049/iet-rsn.2010.0375
Zyl, J. J. V. (2011). Synthetic Aperture Radar Polarimetry: Wiley.

Citation: Ahmad, E. Z., Bahman, Z., Manoochehr, N. (2018). Reconstruction of compressive sensing-based SAR imaging using Nesterov's algorithm. *Ukrainian Journal of Ecology, 8*(3), 154-163.